Validation of nonlinear finite element model of reinforced concrete beams subjected to monotonic loading

Jimmy Chandra[1*], *Yonathan Billy* Christian[1], *Felix Go* Ardenlie[1], *Hartanto* Wibowo[2]

[1]Civil Engineering Department, Faculty of Civil Engineering and Planning, Petra Christian University, Jl. Siwalankerto 121-131, Surabaya 60236, Indonesia

[2]Department of Civil, Construction, and Environmental Engineering, Iowa State University, 813 Bissell Road, Ames, Iowa, United States of America

Abstract. The nonlinear behavior of reinforced concrete beams is complex due to their heterogenic properties and crack formations. Thus, a more accurate estimation through experimental testing and nonlinear finite element modeling is necessary to understand better such behavior. Experimental testing of a reinforced concrete beam subjected to monotonic loading was conducted in laboratory. The test specimen along with seven specimens from various literature were then modeled and analyzed using VecTor2 software to investigate the capability of the software in predicting the load-displacement curves and crack patterns of the specimens. The analysis results show that the finite element model used in VecTor2 software is able to predict well the load-displacement curves and crack patterns of the specimens failing in flexure and shear mechanisms.

1 Introduction

Reinforced concrete (RC) beam behavior can be regarded as fairly linear if subjected to small loading. However, as soon as cracks are formed, the behavior of RC beam becomes highly nonlinear as the loading increases. This characteristic largely influences the beam structural behavior and failure mode [1]. Understanding and predicting the behavior and strength of RC beam can be crucial in an effort to carry out a better design. Therefore, building code has provided specific requirements for the structural element to withstand various loading conditions.

Experimental testing and numerical validation can be done to predict RC beam strength and nonlinear behavior. Experimental testing is conducted to investigate parameters such as the strength and failure mode of the designed RC beam. A numerical validation with respect to the experimental test data is needed to further investigate the accuracy of the numerical model to predict RC beam behavior. Along with the development of computer technology and the number of experimental database that are increasingly available, numerical modeling can now be carried out more frequently to further confirm its capability to accurately predict the nonlinear behavior of RC beam.

Numerical modeling can be done by using micro modeling and macro modeling. Micro modeling used the Distributed Plasticity Model (DPM), while macro modeling used the Concentrated Plasticity Model (CPM). Micro modeling can produce more accurate results than macro modeling as in DPM, the fiber sections are distributed along the length of the member creating an element-level relationship. On the other hand, CPM applied an elastic element with two nonlinear springs at both ends [2]. Consequently, micro modeling requires a longer computational time than macro modeling to analyze the structural element [3].

In this study, the modeling of several RC beams was done with the aid of VecTor2 software [4]. VecTor2 is a suite software program created for finite element analysis of two-dimensional RC membrane structures based on Modified Compression Field Theory (MCFT) developed by Vecchio and Collins [5] and the Disturbed Stress Field Model (DSFM) by Vecchio [6]. VecTor2 models cracked concrete as an orthotropic material with smeared, rotating cracks [7], and can predict the nonlinear load-displacement response of RC structural elements subjected to static monotonic loading. The aim of this study is to investigate VecTor2 capabilities and limitations in predicting the nonlinear responses of RC beams in terms of load-displacement curves and crack patterns. The results from VecTor2 analyses will be compared to experimental results of RC beams subjected to monotonic loading.

2 Experimental program

A RC beam (labeled as DU1) was tested at the Structural Engineering Laboratory of Petra Christian University, Indonesia. The beam has a rectangular cross-section of 300 mm wide by 600 mm deep. The concrete cover of the beam is 40 mm on all sides. The longitudinal reinforcements of the beam consist of two D19 bars at the top, four D19 bars at the bottom, and two D13 bars

---

*Corresponding author: chandra.jimmy@petra.ac.id

at the mid-depth of the beam. The transverse reinforcements used are D10 bars placed at 100 mm spacing to avoid shear failure as the beam was designed to fail in flexure.

The specimen was simply supported and tested in four-point bending, as shown in Fig. 1. The clear span of the beam is 3000 mm, with two concentrated loads being placed about the midspan of the beam. The distance between the two loads is 600 mm, and hence the shear span ratio of the beam (a/d) is 2.14. The displacements were measured using five Linear Variable Displacement Transducers (LVDTs) and the midspan displacement was used to construct the load-displacement curve of the beam.
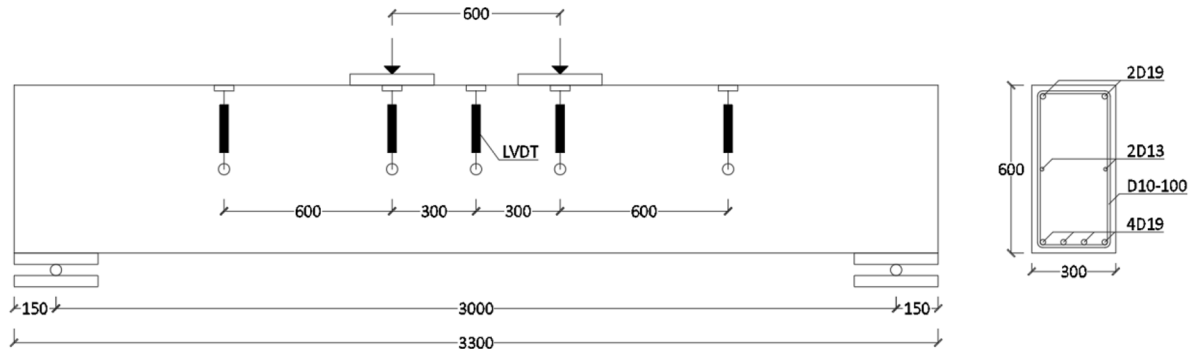
Fig. 1. Loading configuration, instrumentation, and details of DU1 specimen tested at Petra Christian University.

3 Past experimental tests on RC beams from literature

The beam specimens modeled in this research were chosen from the experimental program and literature.

The specimens presented herein consist of DU1 from the experimental program, L1 [8], CON_R8 [9], BN [10], F2 and G2 [11-12], and SB40 and SB42 [13]. The properties of each specimen can be seen in Table 1.

Table 1. Specimen properties of RC beams from the literature.

Specimen	Failure Mode	Size (mm²)	f'_c (MPa)	f_y (MPa)			ρ (%)			
				ts	bs	ms	ts	bs	ms	vsr
DU1	Flexure	300x600	26.40	484	484	520	0.34	0.67	0.16	0.52
L1	Flexure	150x250	26.15	445	445	445	0.32	0.96	0	0.38
CON_R8	Flexure	200x300	21.40	440	440	440	0.19	1.34	0	0.67
BN	Flexure	150x250	24.30	427	427	427	0.51	0.77	0	0.38
F2	Shear	100x400	60.60	404	364	557	0.69	3.66	0.17	0.67
G2	Shear	100x400	30.50	404	364	557	0.69	3.66	0.17	0.59
SB40	Shear	150x250	43.44	500	500	500	0.17	1.35	0	0
SB42	Shear	150x250	42.16	500	500	500	0.17	1.35	0	0

Note:
ts = top steel reinforcement
bs = bottom steel reinforcement
ms = middle steel reinforcement
vsr = vertical shear reinforcement ratio

4 Modeling

4.1 Material

In this analysis, the Hognestad (parabola) available in VecTor2 was used as the basic model for the pre-peak region to the concrete's peak point (ε_p, f_p) of compression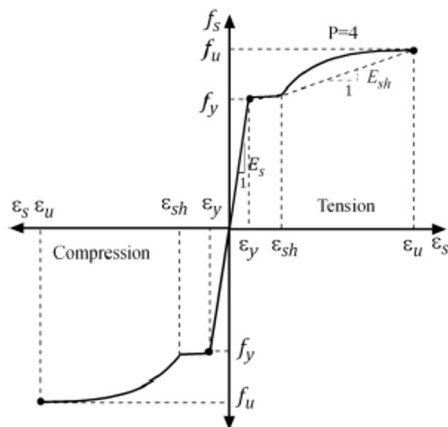 stress-strain curve relationship as shown in Fig. 2(a). To model the post-peak region of the curve in this analysis, the Modified Kent-Park model [14-15] that is available in VecTor2 was used as the basic model. In this model, the first part of the compression stress-strain curve is the Hognestad model (parabola) based pre-peak region, where the peak point (ε_p, f_p) is defined as (0.002, f'_c) for unconfined concrete. For confined concrete, the strength increase due to confinement (K) is considered, and the peak point becomes (0.002K, Kf'_c). The second

part of the curve is a linear descending branch as shown in Fig. 2(b).

(a)   (b)
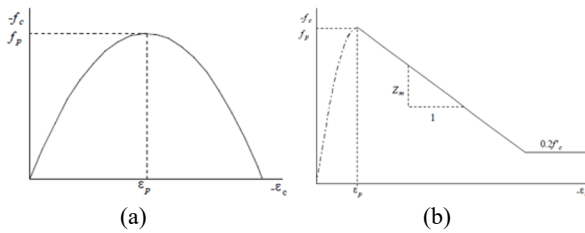
Fig. 2. (a) Hognestad model (parabola) for pre-peak concrete stress-strain curve in VecTor2 [7], (b) Modified Kent-Park for post-peak concrete stress-strain curve in VecTor2 [7].

The stress-strain relationship available in VecTor2 for modeling the response of ductile steel reinforcement has three phases. The three phases consist of the initial elastic response, yielding plateau, and strain-hardening phase as shown in Fig. 3. The value of the strain-hardening parameter (P) can be equal to 1 (linear strain hardening phase; trilinear response) or equal to 4 (nonlinear strain hardening phase; HP4 response). By default, the VecTor2 setting opted for 4 for the value of P, which was used in this analysis.

Fig. 3. Steel HP4 stress-strain curve [7].

4.2 Specimen

The specimens were modeled as two-dimensional reinforced concrete membrane structures in the program. In this study, the longitudinal reinforcements were modeled as discrete reinforcements, whereas the transverse reinforcements were modeled as smeared reinforcements. The maximum rectangular mesh size of every model used in this study was 50 mm. For specimens having different spacings of transverse reinforcement or unconfined regions in the midspan, the material models were also applied differently in the program, visually indicated by different colors. The concrete clear cover regions of the beams were applied as unconfined concrete regions.

The load was applied as displacement-controlled loading. The total applied force and the displacement of the beams were collected to construct the load-displacement curves, which would be compared to those obtained from the experiments. The crack pattern of the beams from the analyses were also compared to those recorded from the experiments. The typical nonlinear finite element model of the specimens in VecTor2 can be seen in Fig. 4.
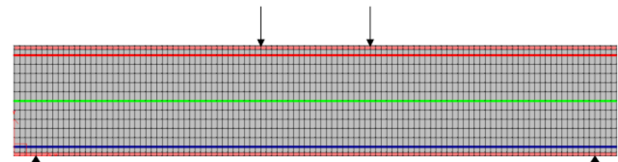

Fig. 4. DU1 specimen model.

5 Results and discussions

The analysis results for the specimens are presented in this section. In the following sections, the term "model" is used to refer to the results of beam analyses using VecTor2. The analysis results in terms of maximum load of the specimens predicted by VecTor2 are summarized in Table 2.

Table 2. The maximum load of the specimens obtained from experiments compared to analytical models.

| Specimen	Failure Mode	Maximum Strength (kN)		Ratio [VecTor2/EXP)
		Experiment (EXP)	**VecTor2**	
DU1	Flexure	580.94	637.93	1.10
L1	Flexure	69.27	67.11	0.97
CON_R8	Flexure	30.30	33.65	1.11
BN	Flexure	53.45	60.31	1.13
F2	Shear	706.00	761.86	1.08
G2	Shear	372.00	354.23	0.95
SB40	Shear	90.60	102.57	1.13
SB42	Shear	271.00	285.69	1.05

5.1 Flexural beams

Fig. 5 shows the comparison of load-displacement curves and crack patterns of the DU1 beam. From the experimental testing results, the DU1 specimen reached its maximum load at 580.94 kN. After that, the load decreased dramatically. The model overestimated the peak load by 10%. The model successfully simulated the strength degradation of the specimen at the end of the loading stages, though the corresponding loads were overestimated. The model estimated the initial stiffness of the specimen quite well as shown in Fig. 5(a).

(a)

(b)
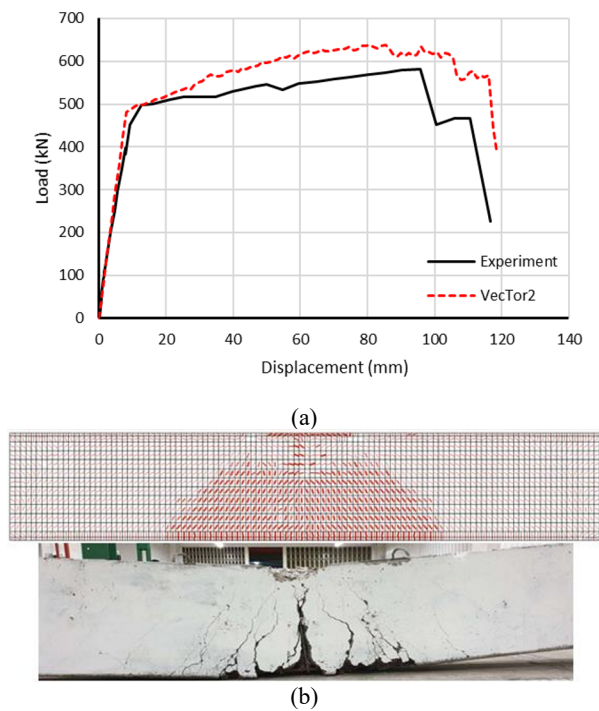
Fig. 5. (a) DU1 load-displacement curves comparison, (b) DU1 crack patterns comparison.

The crack pattern from the experimental testing was governed by the flexural cracks concentrated at the midspan of the specimen as shown in Fig. 5(b). The model predicted the crack pattern quite well. It can be seen that the model predicted a similar pattern where the cracks were concentrated in the midspan region.

Fig. 6-8 show the comparisons of the load-displacement curves and crack patterns of the L1 [8], CON_R8 [9], BN [10] beams. The models underestimated the peak load of L1 by 3% but overestimated the peak load of CON_R8 and BN by 11% and 13%, respectively. The models predicted the initial stiffness of L1 and CON_R8 well but underestimated the initial stiffness of BN as well as overestimated the post-cracking stiffness of L1. Furthermore, the models could not simulate the strength degradation of L1 and CON_R8 by the end of the loading stages as shown in Fig. 6(a) and Fig. 7(a). However, the models could predict the major flexural cracks that were concentrated at the midspan quite well for the three beams as shown in Fig. 6(b)-8(b).
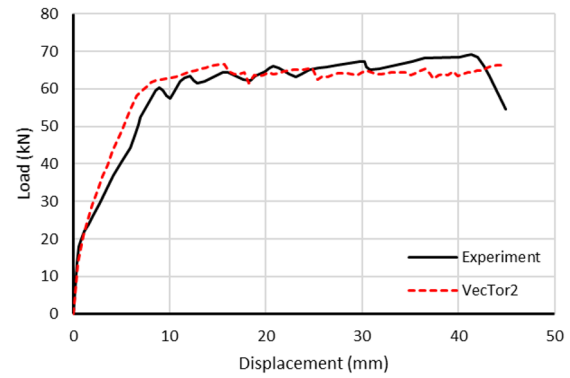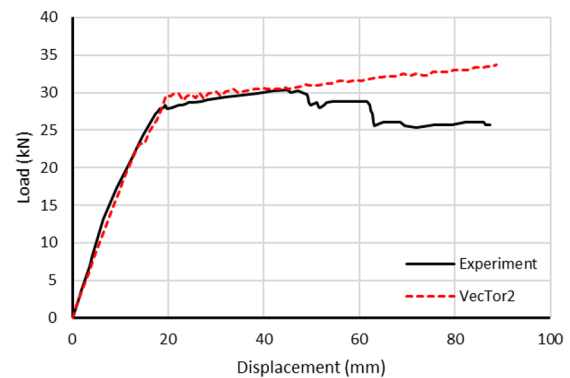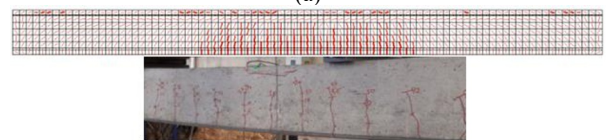

(a)
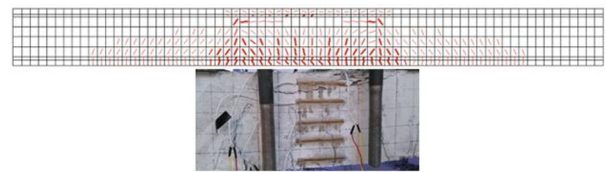
(b)

Fig. 6. (a) L1 load-displacement curves comparison, (b) L1 crack patterns comparison [8].


(a)

(b)

Fig. 7. (a) CON_R8 load-displacement curves comparison, (b) CON_R8 crack patterns comparison [9].

5.2 Shear beams

Fig. 9-12 show the comparisons of load-displacement curves and crack patterns of the experimental tests and analytical models for specimens F2 and G2 [11, 12], and SB40 and SB42 [13]. The models overestimated the peak load of F2, SB40, and SB42 by 8%, 13%, and 5%, respectively but underestimated the peak load of G2 by 5%. Moreover, the models predicted the initial stiffness well for F2 and SB42 but slightly underestimated the initial stiffness for G2 and SB40.

Specimen F2 failed in a shear mechanism indicated by the concrete strut crushing near the support and specimen G2 failed in a shear-compression mechanism indicated by the concrete nodal zone crushing at the

point of loading and near the support. The models failed to simulate the major cracks on the two beams particularly concentrated major cracks indicating crushing as shown in Fig. 9(b) and Fig. 10(b). Specimens SB40 and SB42 failed in a shear mechanism indicated by the major cracks propagating from the support to the point of loading. For both SB40 and SB42 beams, the models could not simulate the major shear cracks as shown in Fig. 11(b) and Fig. 12(b), and the flexural cracks were shown faintly on the beam midspan.
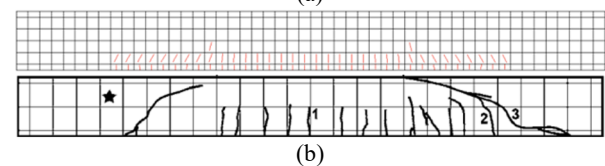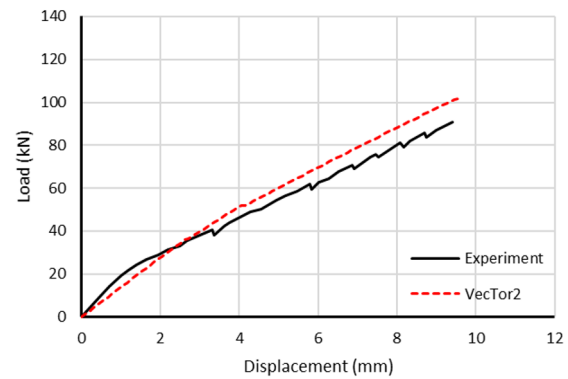

(a)

(b)
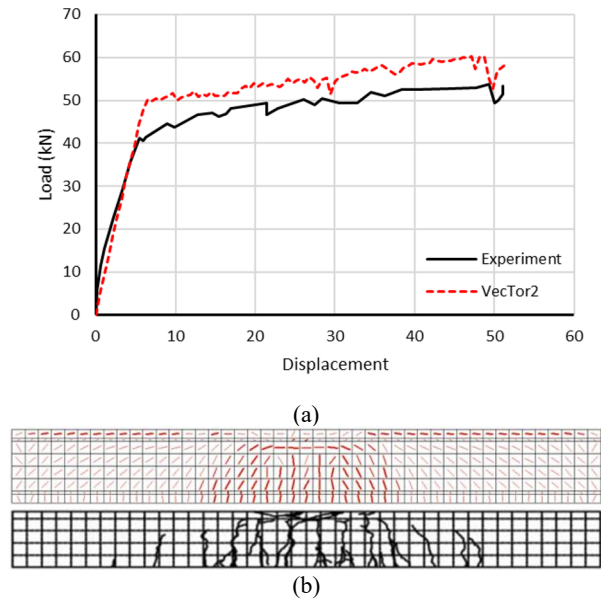
Fig. 8. (a) BN load-displacement curves comparison, (b) BN crack patterns comparison [10].

(a)

(b)
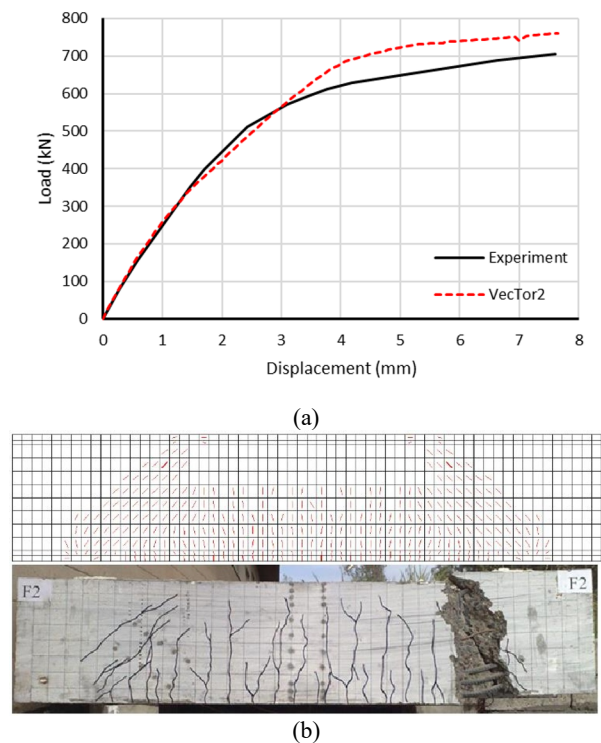
Fig. 9. (a) F2 load-displacement curves comparison, (b) F2 crack patterns comparison [11-12].

(a)

(b)
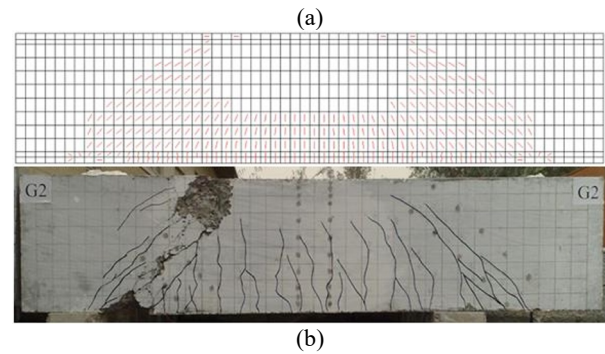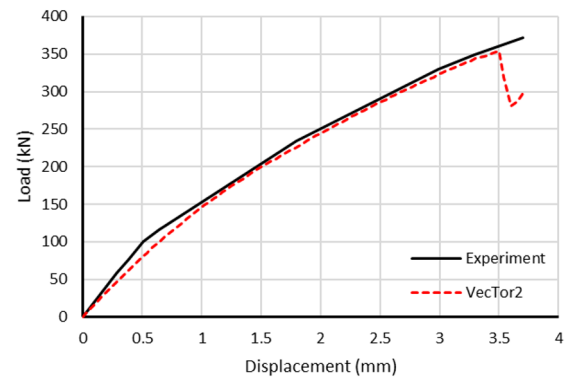
Fig. 10. (a) G2 load-displacement curves comparison, (b) G2 crack patterns comparison [11-12].


(a)

(b)

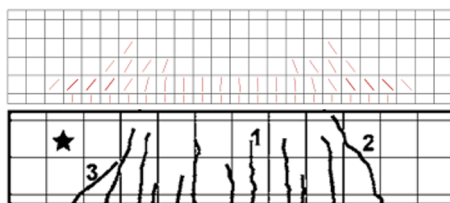**Fig. 11.** (a) SB40 load-displacement curves comparison, (b) SB40 crack patterns comparison [13].

6 Conclusions

Four RC beam specimens failing in flexure mechanism and four RC beam specimens failing in shear mechanism have been modeled and analyzed using VecTor2 software. It can be concluded that in general, VecTor2 can estimate the peak load of the specimens well. The differences between experimental and analytical results are below 15% for all specimens failing in flexure and shear mechanisms. However, VecTor2 that is based on MCFT and DSFM tends to overestimate the peak loads as shown in Table 2.

Furthermore, Vector2 is able to predict the crack patterns quite well for specimens failing in flexure. Nevertheless, the software sometimes cannot display major cracks in specimens failing in shear. Moreover, the strength degradation of some specimens was also poorly predicted. Overall, it can be concluded that VecTor2 can predict reasonably well the structural responses of RC beams subjected to monotonic loading.
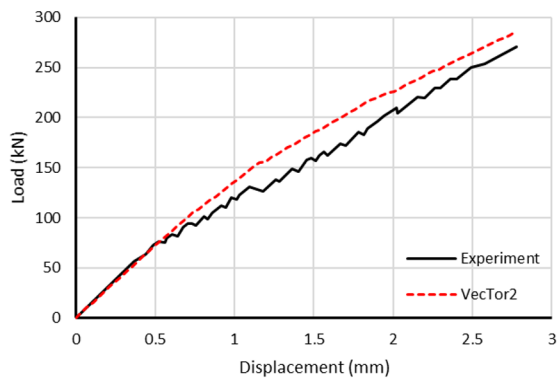
(a)

(b)

Fig. 12. (a) SB42 load-displacement curves comparison, (b) SB42 crack patterns comparison [13].

References

1. P. Bernardi, R. Cerioni, E. Michelini, Procedia Structural Integrity **2**, 2873-2880 (2016) https://doi.org/10.1016/j.prostr.2016.06.359

2. M.F. Giberson, Journal of the Structural Division **95**(2), 137-157 (1969) https://doi.org/10.1061/JSDEAG.0002184

3. A. Calabrese, J.A. Almeida, R. Pinho, Journal of Earthquake Engineering **14**(Sup 1), 38-68 (2010) https://doi.org/10.1080/13632461003651869

4. F.J. Vecchio, VecTor2 basic, Computer software (2021) http://vectoranalysisgroup.com/software.html

5. F.J. Vecchio, M.P. Collins, ACI Journal **83-22**, 219-231 (1986)

6. F.J. Vecchio, Journal of Structural Engineering **126**(9), 1070-1077 (2000) https://doi.org/10.1061/(ASCE)0733-9445(2000)126:9(1070)

7. P.S. Wong, F.J. Vecchio, H. Trommels, VecTor2 and formworks user's manual 2nd edition (University of Toronto, Canada, 2013)

8. Y. Deng, Z. Li, H. Zhang, A. Corigliano, A.C.C. Lam, C. Hansapinyo, Z. Yan, Composite Structures **257**, 113385 (2021) https://doi.org/10.1016/j.compstruct.2020.113385

9. T.N.S. Billows, A. Rteil, Symposium Paper **327**, 30.1-30.14 (2018) DOI: 10.14359/51713351

10. Y. Bahn, R.S. Harichandran, Journal of Composites for Construction **12**(4), 387-395 (2008) https://doi.org/10.1061/(ASCE)1090-0268(2008)12:4(387)

11. K.S. Ismail, M. Guadagnini, K. Pilakoutas, Structural Journal **114**(1), 87-99 (2017) DOI: 10.14359/51689151

12. K.S. Ismail, Doctoral dissertation, University of Sheffield (2016) https://etheses.whiterose.ac.uk/12600/1/Thesis-white%20rose.pdf

13. M. Guadagnini, K. Pilakoutas, P. Waldron, Journal of Composites for Construction **10**(6), 464-473 (2006) https://doi.org/10.1061/(ASCE)1090-0268(2006)10:6(464)

14. D.C. Kent, R. Park, Journal of the Structural Division **97**(7), 1969-1990 (1971) https://doi.org/10.1061/JSDEAG.0002957

15. R. Park, N. Priestley, W.D. Gill, Journal of the Structural Division **108**(4), 929-950 (1982) https://doi.org/10.1061/JSDEAG.0005933